A micromachined freestanding terahertz absorber with an array of metallic patches

Hamdi Torun,[1,2,a] Seyedehayda Sadeghzadeh,[1] Habib Bilgin,[1] and Arda D. Yalcinkaya[1,2]
[1]*Department of Electrical and Electronics Engineering, Bogazici University, Bebek 34342 Istanbul, Turkey*
[2]*Center for Life Sciences and Technologies, Bogazici University, Kandilli 34684 Istanbul, Turkey*

(Received 19 January 2016; accepted 22 March 2016; published online 30 March 2016)

An array of square metallic patches on a thin suspended dielectric layer is introduced as an effective terahertz absorber. The suspended structure is placed on a metalized substrate and the device exhibits metamaterial behavior at specific frequencies determined by the size of the patches. It is feasible to place patches with different sizes in an array formation for a broadband absorber. In array configuration, individual elements induce distinct resonances yielding narrow band absorption regions. Design of the absorber is described using electromagnetic simulations. The absorber structure was fabricated on a silicon wafer using standard microfabrication techniques. The characteristics of the absorber were measured using a terahertz time domain spectroscope. The measured data match well the simulations indicating strong absorption peaks in a band of 0.5-2 THz. [http://dx.doi.org/10.1063/1.4945417]

I. INTRODUCTION

Metamaterials are patterned sub-wavelength sized structures that are usually made of dielectrics and metals. They exhibit strong resonant behavior when they are excited with electromagnetic waves and the resonant frequencies are determined by the geometries of the patterned structures. Metamaterials with different geometries and sizes have been introduced for a wide range of bands in electromagnetic spectrum spanning from radio[1–3] to terahertz,[4] infrared[5] and visible frequencies.[6] The wavelength of the radiation at 1 THz corresponds to 300 μm, so it is feasible to fabricate metamaterial structures for terahertz applications using standard UV photolithography. In addition, most of the materials used for the realization of metamaterials are compatible with microfabrication technology. Consequently, a wide variety of metamaterial microstructures have been presented for terahertz applications. Variety of imaging and spectroscopy applications in terahertz band has been increasing rapidly including detection of explosives,[7] surveillance,[8,9] chemical sensing,[10] and medical screening.[11,12] High performance terahertz absorbers enable developing new devices for these applications.

Metamaterial-based terahertz absorbers have been employed that exhibit a magnetic or electric resonance at desired frequencies. Different geometries have been demonstrated including split-ring resonators,[13,14] Swiss crosses,[15–17] concentric rings,[18] square patches,[19–23] and circular disks.[24] At resonance, these structures can absorb radiation with high efficiency. Unity absorption is observed with metamaterial absorbers at terahertz frequencies.[25] However, the absorption band is usually very narrow. For example, the full width at half maximum (FWHM) of the absorption peak is 0.1 THz for an absorber at 1 THz.[25] Typically, structures with different sizes are combined together to increase the number of absorption bands for broadband absorbers. As an alternative method,

[a]Corresponding author. Tel: +90 212 359 68 95. E-mail address: hamdi.torun@boun.edu.tr

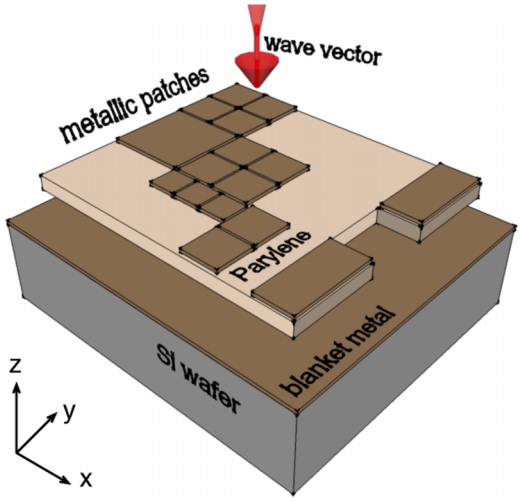

FIG. 1. Three-dimensional drawing of the metamaterial-based terahertz absorber structure.

square patches with comparable sizes are located in a planar array[19] or are stacked on top of each other with dielectric spacers in between[20,23] to increase the number of absorption bands. In addition, concentric rings are used as resonators to extend the absorption band as well.[18]

In this paper, we present a metamaterial-based terahertz absorber employing metallic square patches implemented in the same plane with different sizes. Fig. 1 shows a three-dimensional drawing of an absorber structure on a silicon wafer. The metallic patches are fabricated on top of a thin patterned Parylene layer that is suspended over a metallized substrate. Terahertz resonators on thin dielectric layers are demonstrated for filter and sensor applications in the literature.[26,27] Our aim is to realize a terahertz absorber on a thin layer of dielectric and the intended configuration for the absorber is when the incident wave vector is perpendicular to the device as shown in Fig. 1. Metallic patches with different sizes are laid out on a single Parylene film that is anchored to the substrate through a set of suspensions. This configuration is desirable for terahertz detectors that requires pixel structures isolated from their substrate. The metamaterial behavior is observed for unit cells including the metallic patches on top, blanket metal on the substrate and the Parylene and air spacing in between. Transmission is guaranteed to be zero with the presence of the thin blanket metal underneath the patches, whereas reflection from the device diminishes at certain frequencies set by the geometry of the square patches, resulting in increased absorption at those frequencies.

We implemented absorbers employing different configurations of square patch arrays made of titanium with side lengths of 86 μm, 43 μm, 30 μm and rectangular patches with side lengths of 100 μm and 43 μm. The individual metal patches are separated by a planar gap of 2 μm. The thickness of the patches and the blanket titanium film underneath the patches is 200 nm. The Parylene layer is implemented in a 2 μm-thick released mesa. The thickness of the air gap between the Parylene layer and the blanket metal is 5 μm.

II. SIMULATIONS AND MODELING

Fig. 2(a) shows a three-dimensional drawing of a metamaterial-based terahertz absorber that includes a 4x4 array of patches with a size of 43 μm at the center of the free-standing Parylene layer. The absorber also includes two rectangular patches with a size of 100x43 μm. Fig. 2(b) shows the reflection, transmission and absorption spectra of the absorber obtained using a commercially available electromagnetic simulation software (CST Studio Suite, Darmstadt, Germany). The propagation vector is normal to the surface (along z-axis, Fig. 1) and the electric field vector is aligned along y-axis of Fig. 1. We implemented waveguide ports perpendicular to the structure as the source of excitation for the simulations and chose a time domain solver with hexahedral adaptive meshing.

The absorption spectrum in a band of 0.3-2 THz exhibits two peaks at 0.59 THz and 1.47 THz. The patch structures introduce electric dipole resonances at specific frequencies induced by the electric field in the plane of the patches. At resonance, the metamaterial can be modeled using a parallel combination of an equivalent capacitance (C_{eq}) and inductance (L_{eq}) given below.[19]

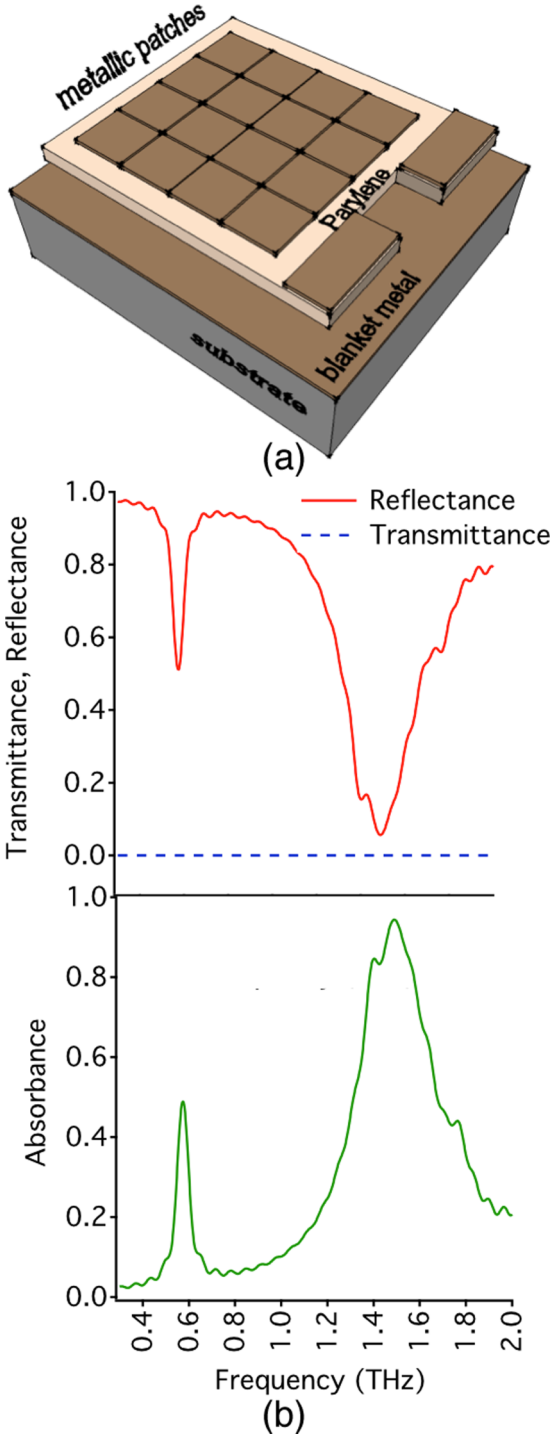

FIG. 2. a) Three-dimensional drawing of a metamaterial-based terahertz absorber with a 4x4 array of patches with a size of 43 μm and two rectangular patches with a size of 100x43 μm. (b) Simulated transmission, reflection and absorption spectra of the absorber.

$$C_{eq} = \frac{\alpha \varepsilon_{eff} L^2}{t_{eff}}, \quad L_{eq} = \beta \mu_{eff} t_{eff} \tag{1}$$

$$f_{res} = \frac{1}{2\pi\sqrt{L_{eq} C_{eq}}} \tag{2}$$

where L is the side length of a square patch, t_{eff} is the effective thickness of the structure between top and bottom metal films, α and β are geometrical correction parameters, ε_{eff} and μ_{eff} are the effective permittivity and permeability of the structure, respectively.

The resonant frequency of the structures is inversely proportional to the size of the patches. The larger rectangular patches excites a resonance at 0.59 THz while the smaller square patches excites

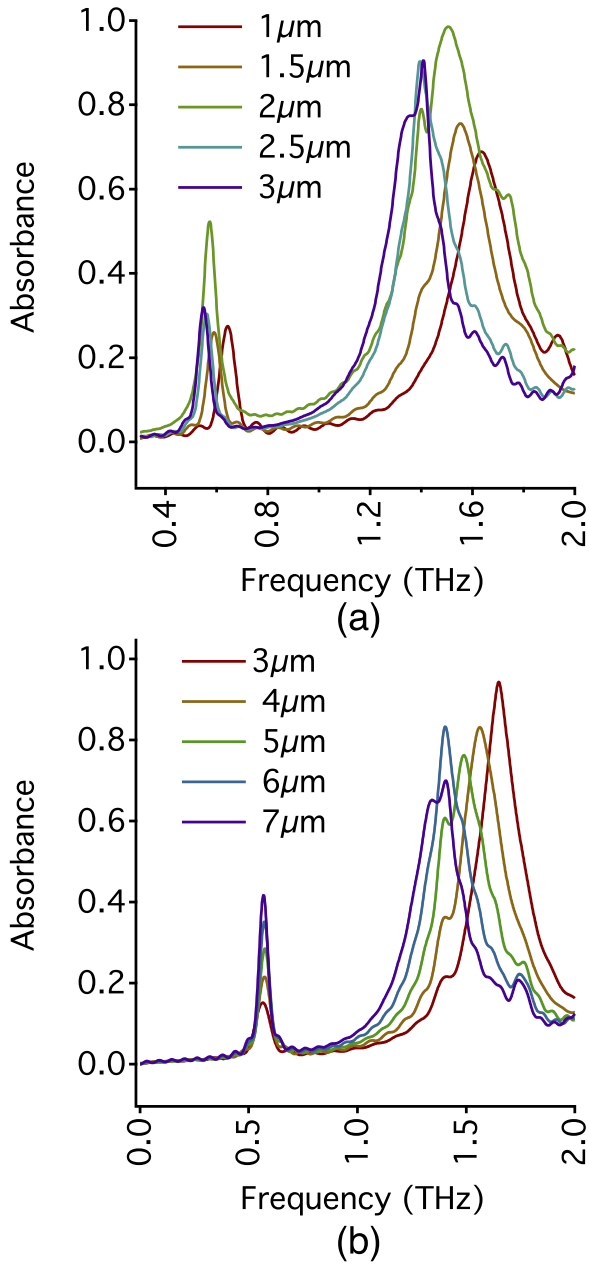

FIG. 3. The variation of the resonance characteristics of the structure as a function of (a) thickness of the Parylene layer, (b) gap height at the tip of the structure.

another resonance at 1.47 THz. The array formation of the square patches enhances the peak of the absorption at the resonance. The resonant frequency of the device is also determined by the effective relative permittivity of the structure. So, the thickness of the Parylene layer has an influence on the resonance characteristics. Fig. 3(a) shows the distribution of the resonance peaks with respect to the changes in the thickness of the Parylene layer. The effective permittivity of the structure increases with the thickness of the dielectric layer. This results in a decrease in resonant frequency of the device, as expected.

During the operation of the device, the freestanding structure will be tilted with respect to its substrate. We analyzed the dependency of the resonator behavior by introducing a tilt angle such that the position of the edge of the structure where we place the rectangular patches is kept stationary and the freestanding structure is tilted about the y-axis (Fig. 1). We varied the gap at the tip of the structure between 3 and 7 μm and observed the resonance characteristics as shown in Fig. 3(b). The resonant frequency of the structure excited by the rectangular patches keeps the same value at 0.59 THz, since the effective gap change along the rectangular patches are minimal. However, the resonant frequency related to the array of the square patches decreases with increasing gap.

The length of the patches along which the electric field is aligned determines the resonant frequency of the structure. Thus, the resonant frequency is ideally the same for the electric field vector aligned along x-axis or y-axis of Fig. 1 since the basic structure is a square. We analyzed the dependency of the resonator characteristics with respect to the polarization as shown in Fig. 4. The field was kept perpendicular to the device along z-axis and we varied the angle β between

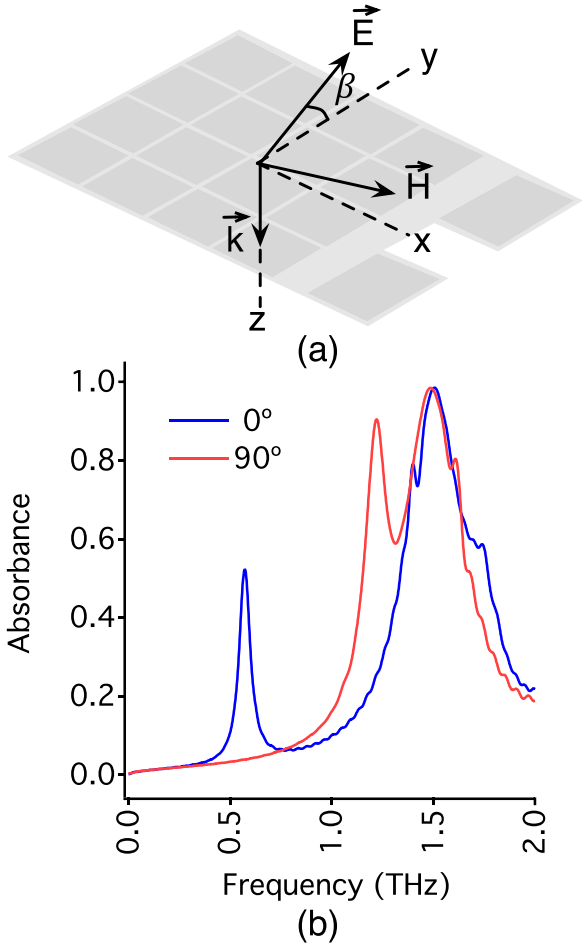

FIG. 4. The dependency of the resonance characteristics of the structure with respect to the orientation of electric field. (a) Variation of the angle between the electric field vector and y-axis. The electric field and the magnetic field vector is in the plane of xy. (b) Absorbance of the structure with different values of β.

the electric field vector and y-axis. The absorption spectra for $\beta = 0°$ and $\beta = 90°$ are shown in Fig 4(b). The resonant frequency of the structure at 1.47 THz due to the square patches is not altered. However, the resonance at 0.59 THz due to the square patches disappears for $\beta = 90°$ since the electric field is no more aligned along the larger side of the rectangular patches. On the other hand, another resonance at 1.2 THz is observed for $\beta = 90°$ as a result of the interaction between the rectangular and square patches at that frequency.

Due to the fact that the resonance is mainly determined by the electric field vector along the edge of a square or a rectangular patch, the incidence angle should have minor influence on the resonance behavior as long as the orientation of the electric field vector is kept the same. We analyzed the influence of the incidence angle for TE mode as shown in Fig. 5(a) by varying the angle θ between the incoming beam and the z-axis. The absorption spectra of the structure for various angles of θ are shown in Fig. 5(b). The structure performs well as an absorber even for large incidence angles for TE mode as expected.

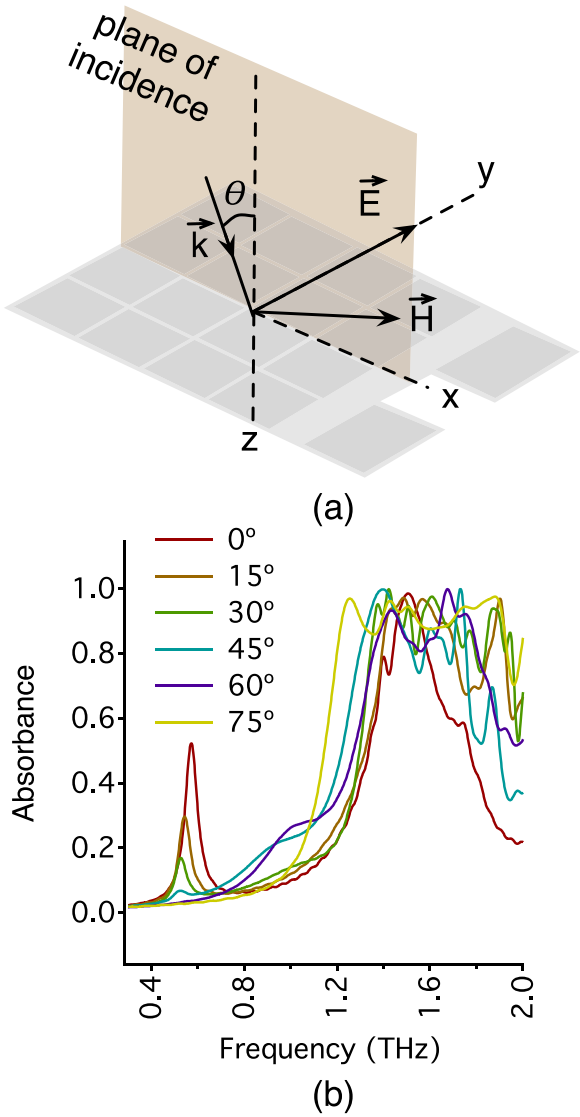

FIG. 5. The dependency of the resonance characteristics of the structure with respect to the incidence angle. (a) The plane of incidence and the angle between the propagation vector and z-axis is shown. The orientation of electric field is stationary and is along y-axis. (b) The dependency of the resonance characteristics of the structure with respect to the changes of the angle θ.

We designed another absorber by combining different sizes of patches on a single freestanding Parylene layer. The layout of the patches is shown in Fig. 1. The absorber includes square patches with side lengths of 86 μm, 43 μm, 30 μm and rectangular patches with side lengths of 100 μm and 43 μm. The computational model for the absorber includes all the structures shown in Fig. 1. Electric field is along y-axis for the simulations. The reflection, transmission and absorption spectra of the absorber are shown in Fig. 6. The absorption spectrum exhibits sharp resonant peaks at 0.63 THz, 1.12 THz, 1.47 THz and 1.87 THz. Compared to Fig. 2, it can be seen that incorporating patches with different sizes improve the absorption characteristics of the device.

Electric field distributions corresponding to the resonant frequencies are shown in Fig. 7. Larger patches are associated with smaller frequencies. Specifically patches with 100 μm side lengths excites resonance at 0.63 THz, 86 μm patch excites resonance at 1.12 THz, 43 μm patches and their interactions with 30 μm patches excite resonance at 1.47 THz. The rectangular patches also excite another resonance at 1.87 THz. The absorber characteristics are different when the electric field is along x-axis (see Fig. 1), since the absorber includes two rectangular patches. The resonant frequency of a specific patch element is proportional to the reciprocal of the side length of the patch.[19] So, the electric field orientation determines the effective side length of a rectangular patch.

Considering the equations (1) and (2), it can be deduced that for an absorbing element, resonant frequency is inversely proportional to L. Simulation results with individual square patch structures verify the dependency of the resonant frequency to the patch size as shown in Fig. 8. The linear fit can be used as a powerful design tool for the absorbers. The wavelength of waves propagating in vacuum at 1 THz is approximately 300 μm. This value sets a limit for the minimum size of structures in a pixelated array form. Fig. 8 shows that it is feasible to fit various combinations of different patch geometries in a typical pixel for the operation wavelength. The analytical model of equation 1 suggests that the resonant frequency is independent of the thickness between the electrodes, t_{eff}. Although the dependency of the resonant frequency with respect to t_{eff} is weak, we observe that the resonant frequency is altered with the tilt of the freestanding structure as shown in Fig. 3(b).

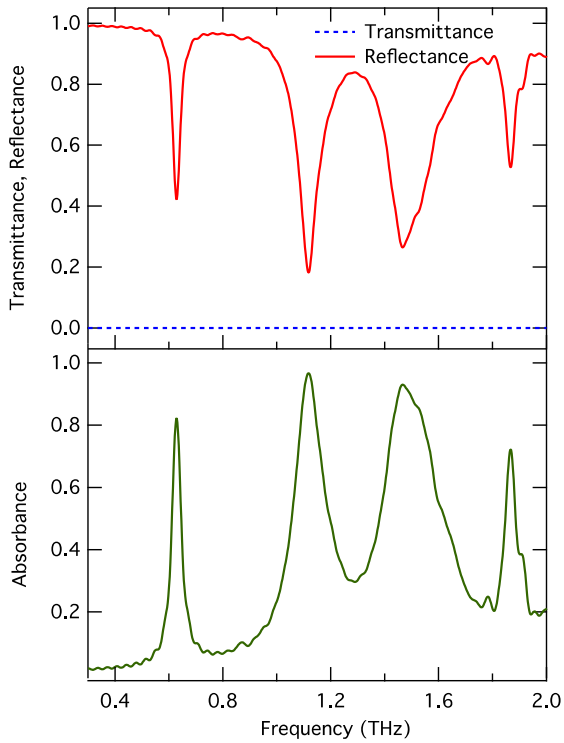

FIG. 6. Simulated transmission, reflection and absorption spectra of the absorber.

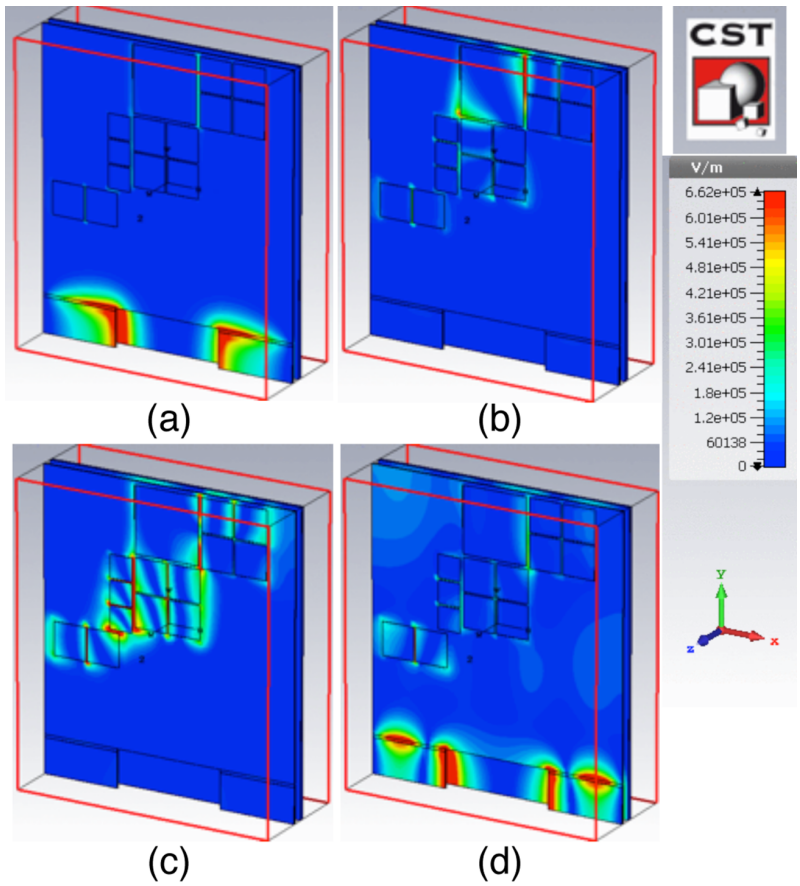

FIG. 7. Distribution of electric field at a) 0.63 THz, b) 1.12 THz, c) 1.47 THz and d)1.87 THz.

III. FABRICATION AND EXPERIMENTAL CHARACTERIZATION

We fabricated the designed absorbers using standard microfabrication methods. An SEM image for a fabricated structure is shown in Fig. 9. The design of this device is shown in Fig. 1. The Parylene layer is anchored to the substrate near to the rectangular patches. The Parylene layer also

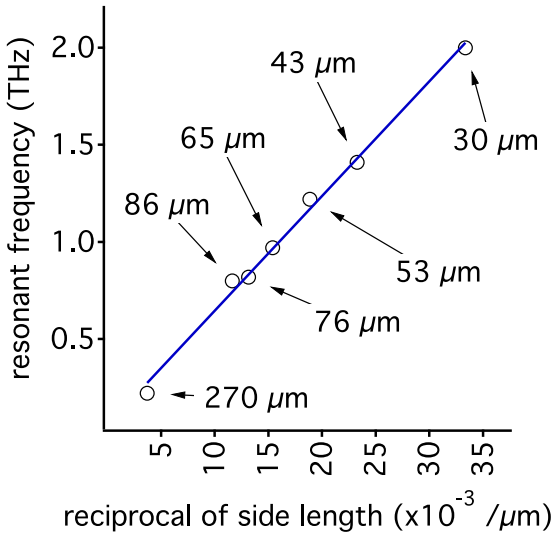

FIG. 8. Dependency of the resonant frequency of square patches as a function of side lengths.

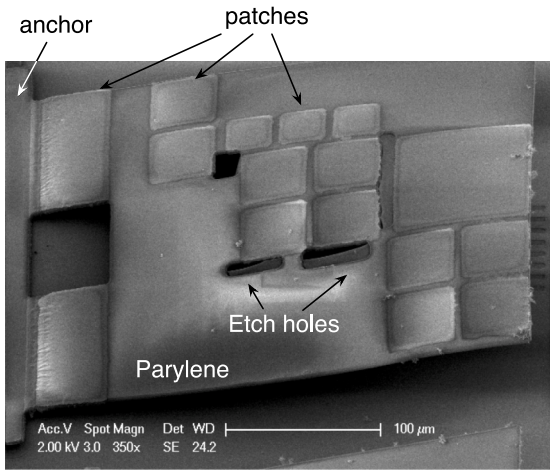

FIG. 9. SEM image of a fabricated absorber.

includes etch holes that helps removing the sacrificial layer underneath the structure during the releasing step using wet etching. We measured the characteristics of the fabricated absorber using a terahertz time-domain spectroscope (TERA K15, Menlo Systems GmbH, Martinsried, Germany). We obtained the transmission and reflection spectra of the absorber using reference measurements and calculated the absorption spectrum as shown in Fig. 10. We collected the data for the case when no sample was placed between the emitter and the receiver antennas of the spectrometer as the reference for the transmission measurements. Then we placed a thick metal reflector between the antennas that are bent 90° to collect the reference measurement for the reflectance measurements.

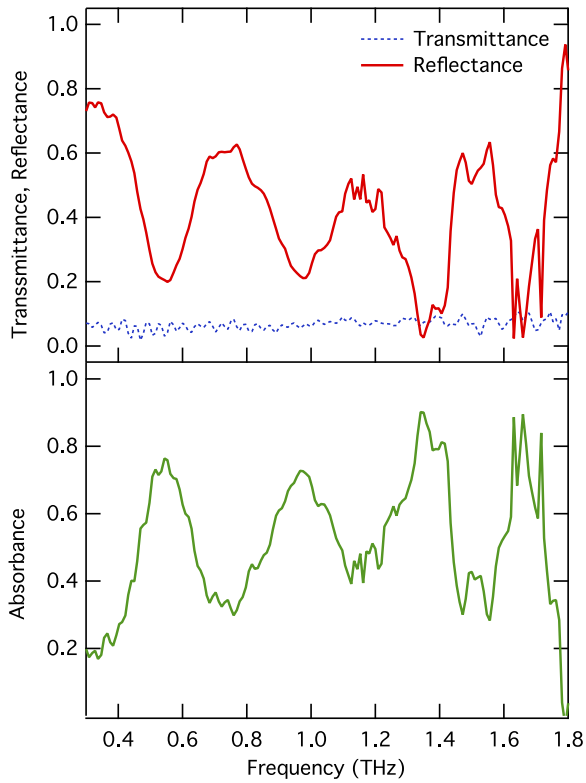

FIG. 10. Measured transmission, reflection and absorption spectra of the absorber.

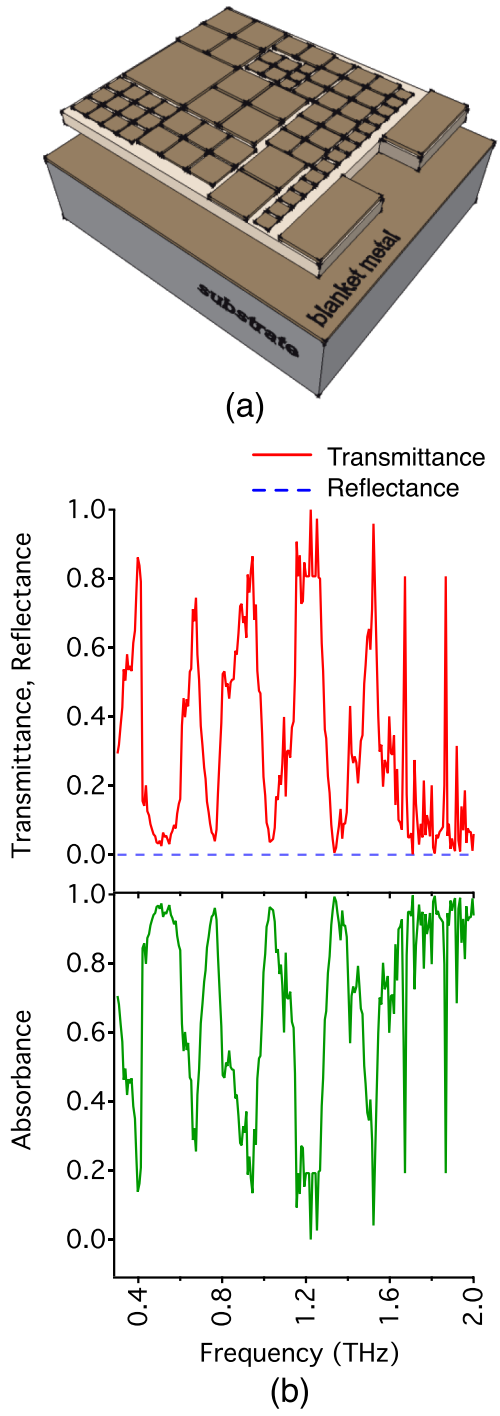

FIG. 11. a) Three-dimensional drawing of a metamaterial-based terahertz absorber with square patches with side lengths of 15, 20, 25, 30, 43 and 86 μm and two rectangular patches with a size of 100x43 μm. (b) Measured transmission, reflection and absorption spectra of the absorber.

The measured absorption peaks match well with the simulated peaks. The measured resonant frequencies exhibit redshift with respect to the simulation results. The largest deviation is observed with the first resonant frequency where the measured frequency is 20% smaller than the simulation results. We identify the sources of the error as the differences between the material properties we used for the simulations and the actual ones, the deviation of the incidence angle from the normal

incidence angle case and the deviation of the polarization of the electric field. Nevertheless, the measurement results verify our findings in simulations.

We fabricated another design that is shown in Fig. 11(a). We obtained this design by filling the empty spaces of the design shown in Fig 1 with different patches. The design includes square patches with side lengths of 15, 20, 25, 30, 43 and 86 μm and two rectangular patches with a size of 100x43 μm. The absorption spectrum shown in Fig. 11 indicates distinct resonances in a band of 0.3-2 THz. We realized a broadband absorber in this design by combining patches with different sizes. The device exhibits significant absorption in this band as a result of the resonances of individual patches and the interactions between patches. We measured zero transmission for this design in the designated band. However, the transmission we measured for the device of Fig. 9 is very small but finite. The most significant difference between two designs is the fill factor considering the patches on the surface of the device. A significant portion of the device of Fig. 9 does not include any patches and the incoming radiation impinges on the Parylene surface, which is transparent. We realize the bottom electrode, which is 200 nm in thickness transmits some of the power it receives contrary to our simulation results. Nevertheless, the transmission is very low (less than 10%) for the entire band for the bottom electrode.

IV. CONCLUSION

An array of square patch metamaterial resonators that can be used as an effective terahertz absorber is presented. We designed square patches with different geometries on a thin layer of Parylene that is suspended over a substrate for a frequency range of 0.5-2 THz. We presented a computational model that explains the resonant absorption characteristics of the device. We analyzed how the behavior of the absorber changes with the polarization and the incidence angle. We fabricated the absorber structure on a Silicon wafer and measured its characteristics at terahertz frequencies using a terahertz time-domain spectroscope. The fabricated device exhibits strong absorption peaks with absorbance of 0.8 at desired frequencies and the absorbance of the device is larger than 0.4 in a band of 0.3-2 THz.

ACKNOWLEDGMENTS

We wish to acknowledge the support of from the Scientific and Technological Research Council of Turkey (TUBITAK) Project 112E250 and Scientific Research Projects (BAP) of Bogazici University Project 8581.

[1] H. Torun, F. C. Top, G. Dundar, and A. D. Yalcinkaya, Journal of Applied Physics **116**, 124701 (2014).
[2] K. Aydin, K. Guven, M. Kafesaki, L. Zhang, C. M. Soukoulis, and E. Ozbay, Optics Letters **29**, 2623 (2004).
[3] D. R. Smith, W. J. Padilla, D. C. Vier, S. C. Nemat-Nasser, and S. Schultz, Physical review letters **84**, 4184 (2000).
[4] T. J. Yen, W. J. Padilla, N. Fang, D. C. Vier, D. R. Smith, J. B. Pendry, D. N. Basov, and X. Zhang, Science **303**, 1494 (2004).
[5] S. Linden, C. Enkrich, M. Wegener, J. Zhou, T. Koschny, and C. M. Soukoulis, "Magnetic response of metamaterials at 100 terahertz," Science **306**, 1351 (2004).
[6] A. Ishikawa, T. Tanaka, and S. Kawata, Physical review letters **95**, 237401 (2005).
[7] K. Yamamoto, M. Yamaguchi, F. Miyamaru, M. Tani, M. Hangyo, T. Ikeda, A. Matsushita, K. Koide, M. Tatsuno, and Y. Minami, Japanese journal of applied physics **43**, L414 (2004).
[8] M. C. Kemp, P. F. Taday, B. E. Cole, J. A. Cluff, A. J. Fitzgerald, and W. R. Tribe, in AeroSense 2003, 44, (2003).
[9] A. W. Lee, Q. Qin, S. Kumar, B. S. Williams, Q. Hu, and J. L. Reno, Applied Physics Letters **89**, 141125 (2006).
[10] L. Liu, R. Pathak, L. Cheng, and T. Wang, Sensors and Actuators B **184**, 228 (2013).
[11] P. C. Ashworth, E. Pickwell-MacPherson, E. Provenzano, S. E. Pinder, A. D. Purushotham, M. Pepper, and V. P. Wallace, Optics express **17**, 12444 (2009).
[12] C. Yu, S. Fan, Y. Sun, and E. Pickwell-Macpherson, Quant Imaging Med Surg **2**, 33 (2012).
[13] H. Tao, C. M. Bingham, D. Pilon, K. Fan, A. C. Strikwerda, D. Shrekenhamer, W. J. Padilla, X. Zhang, and R. D. Averitt, Journal of physics D: Applied physics **43**, 225102 (2010).
[14] Q. -Y. Wen, H. -W. Zhang, Y. -S. Xie, Q. -H. Yang, and Y. -L. Liu, Applied Physics Letters **95**, 241111 (2009).
[15] Y. Q. Ye, Y. Jin, and S. He, JOSA B **27**, 498 (2010).
[16] J. Fu, W. Chen, B. Lv, L. Zhu, and Q. Wu, Solid State Communications **204**, 5 (2015).
[17] J. Grant, Y. Ma, S. Saha, A. Khalid, and D. R. Cumming, Opt Lett **36**, 3476 (2011).
[18] Y. Ma, Q. Chen, J. Grant, S. C. Saha, A. Khalid, and D. R. Cumming, Opt Lett **36**, 945 (2011).
[19] Y. Cheng, Y. Nie, and R. Gong, Optics & Laser Technology **48**, 415 (2013).

[20] B. -X. Wang, L. -L. Wang, G. -Z. Wang, W. -Q. Huang, X. -F. Li, and X. Zhai, Applied Physics A **115**, 1187 (2014).
[21] A. Sellier, T. V. Teperik, and A. de Lustrac, Opt Express **21**, A997 (2013).
[22] F. Alves, B. Kearney, D. Grbovic, N. V. Lavrik, and G. Karunasiri, Applied Physics Letters **100**, 111104 (2012).
[23] B. -X. Wang, L. -L. Wang, G. -Z. Wang, W. -Q. Huang, X. -F. Li, and X. Zhai, Photonics Technology Letters, IEEE **26**, 111 (2014).
[24] G. Dayal and S. A. Ramakrishna, Journal of Optics **15**, 055106 (2013).
[25] D. Y. Shchegolkov, A. K. Azad, J. F. OHara, and E. I. Simakov, Physical Review B **82**, 205117 (2010).
[26] Y. Chen, I. A. Al-Naib, J. Gu, M. Wang, T. Ozaki, R. Morandotti, and W. Zhang, AIP Advances **2**, 022109 (2012).
[27] H. Tao, A. C. Strikwerda, M. Liu, J. P. Mondia, E. Ekmekci, K. Fan, D. L. Kaplan, W. J. Padilla, X. Zhang, and R. D. Averitt, Applied Physics Letters **97**, 261909 (2010).